TINY-SIZED ULTRA-SENSITIVE INFRARED-THERMOPILE FABRICATED WITH A SINGLE-SIDED BULK-SILICON MICROMACHINING TECHNIQUE

Wei Li, Zao Ni, Fang Chen, Jiachou Wang, Fei Feng, and Xinxin Li

State Key Laboratory of Transducer Technology, Shanghai Institute of Microsystem and Information Technology, Chinese Academy of Sciences, 865 Changning Road, Shanghai 200050, CHINA

ABSTRACT

This paper reports a tiny-sized (140μm×140μm) p-Si/Al infrared (IR) thermopile, which is low-cost bulk-micromachined only from the front-side of (111) wafer for IC-foundry compatible manufacturing. With the novel single-side bulk-micromachined structure, the tiny-size MEMS thermopile consists of six single-crystalline (SC) Si/Al thermocouples that show significantly higher Seebeck-coefficient and lower noise compared to the traditional poly-Si/Al thermocouples. The testing results show that the tiny-sized thermopile achieves an ultra-high responsivity of 356V/W and ultra-short response-time of 0.59ms.

INTRODUCTION

Operated at room temperature, thermal IR detectors can respond to a wide range of IR radiation, thereby the devices are suitable for various applications. As one type of thermal detectors, thermopiles have attractive advantages compared with other thermal detectors. Based on the intrinsic self-generating Seebeck effect, thermopiles do not require biasing and, thus, do not need electric-excitation that helps to avoid self-heating effect. Moreover, thermopiles are operated in dc sensing mode. In this way chopper is not needed and the very simple signal readout simplifies the system design. Bearing so many fascinating characteristics, thermopiles have been widely used in various IR detection applications, especially in non-contact heat/temperature measurement. On the other hand, thermopile arrays can expand the usefulness in other areas, including security systems and monitoring to industrial process, by detecting line and plane information rather than spot information [1].

In order to develop miniaturized IR-thermopile for portable detector for human-body and heat monitoring, the device is expected to be adequately small in size but sensitive enough to improve minimum detectable signal. Normally a micromachined thermopile device consists of an insulating thin-film for IR absorbing, several series-connected thermocouples array in the thin film and a free-space under the thin film for effective heat insulation. In the traditional thermopile detector structure, normally poly-Si/metal thermocouple (with low Seebeck coefficient) was integrated on the absorbing thin-film like SiN. Such traditional structure suffers low sensitivity. To solve this problem, so far many methods have been developed to increase sensitivity. One proposed method [2] was by expanding the size of the IR absorbing film. Obviously the method is not helpful for miniaturization of the device for portable applications. Another notable method reported in the work of Ref. [3] used vacuum packaging to enhance the heat insulation of the thermopile detector. Unfortunately, result in much longer response time of thermopiles.

In this paper, a novel-structure tiny-sized (140μm×140μm) SC silicon/Al IR thermopile based on bulk-silicon micromachining technique only from the front-side of (111) wafer is designed, fabricated and characterized. Thanks to the single-side bulk-micromachined novel structure, the tiny-sized MEMS thermopile consists of six SC Si/Al thermocouples that feature significantly higher Seebeck coefficient, lower resistivity and noise compared to traditional poly-Si/Al thermocouples. Thereby our tiny-sized thermopile achieves an ultra-high responsivity of 356V/W and ultra-short response time of 0.59ms in the air.

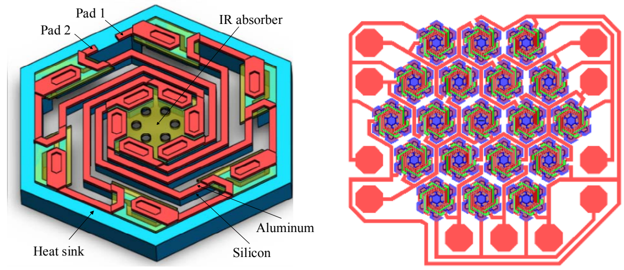

(a) *(b)*

Figure 1: (a) 3D schematic of the bulk-micromachined thermopile. (b) Layout of a 19-pixel arrayed IR detector that can be adapted into a small diameter len.

DESIGN AND FABRICATION

Theoretic analysis

Figure 1(a) shows the schematic of front-side micromachined thermopile IR detector that consists of six series-connected p-Si/Al thermocouples. The six hot-junctions encircle the central IR absorbing SiN thin film. The central SiN thin film is sandwiched between the suspended silicon beams and aluminum wires, with via holes opened in the SiN thin film for the silicon-Al junctions. Under IR exposure, the absorber converts the incident IR radiation to a temperature increase near the hot-junctions. Excellent thermal insulation is achieved by removing the bulk silicon under the absorber and the hot-junctions by bulk-micromachining process implemented only from the front-side of (111) wafer.

According to Seebeck effect theory, the thermopile output voltage ΔV can be expressed as

$$\Delta V = N\alpha_{12}\Delta T \tag{1}$$

where N is number of the thermocouples, α_{12} is the difference of Seebeck coefficient between the two thermoelectric materials and ΔT is the temperature different between the hot and cold terminals. In Ref. [4], ΔT is given as

$$\Delta T = \eta R_{th}\phi_0 A_S \tag{2}$$

where η is the absorption coefficient of the absorber, A_S is sensitive area of the thermopile detector, ϕ_0 is the input IR radiation flux and R_{th} is thermal resistance that comes from the thermopile structure, gas convection and radiation [5].

Table 1: Seebeck coefficient of different materials [6].

Material	Seebeck coefficient (μV/K)
Antimony	+48.9
Chromel	+29.8
Tungsten	+11.2
Gold	+7.4
Copper	+7.6
Silver	+7.4
Aluminum	+4.2
p-Silicon, ρ=0.0035 Ωcm	+450
p-Germanium, ρ=0.0083Ωcm	+420
Platinum	0
Calcium	-5.1
Nickle	-14.5
Bismuth	-73.4
n-Silicon, ρ=0.0035 Ωcm	-450
n-Germanium, ρ=0.69Ωcm	-548

The responsivity of the thermopile IR detector can be calculated as

$$R_V = \frac{\Delta V}{\phi_0 A_S} = \eta N \alpha_{12} R_{th} \tag{3}$$

Indicating signal-to-noise ratio of the thermopile and normalized by the detector size and noise bandwidth, the specific detectivity D*, can be expressed as

$$D^* = \frac{R_V\sqrt{A_S \Delta f}}{u_{noise}} \tag{4}$$

where Δf is the noise bandwidth and u_{noise} is the noise voltage of the thermopile. Because Johnson noise dominates the noise of the thermopile, u_{noise} can be written as

$$u_{noise} = \sqrt{4kTR\Delta f} \tag{5}$$

where k is the Boltzmann-constant, R is the electric resistance of the thermopile detector and T is the environmental absolute temperature.

Response time is another important performance parameter of the detector. For thermopile style detector, the response time is limited mainly by the thermal time constant as

$$\tau = C_{th} R_{th} \tag{6}$$

where C_{th} is thermal capacitance of the structure.

Design optimization

The primary consideration in design of a thermopile detector lies in material selection for the thermocouple hot-junction. According to the above-given theoretic analysis, the chosen thermocouple materials should have as large difference of Seebeck coefficient as possible to achieve high responsivity. Typically, the Seebeck coefficients of semiconductors are much higher than those of metals, as is listed and compared in Table 1. Besides, the Seebeck coefficient of a semiconductor can be adjusted by varying impurity doping concentration. Along with the impurity concentration decreases, the Seebeck coefficient increases, so as the resistivity [7]. However, the resistance of the thermopile limits the minimum detectable signal level because of its thermal noise. It is necessary to optimize the impurity concentration to obtain an appropriate compromise between Seebeck coefficient and thermopile resistance. Since single-crystalline (SC) silicon features significantly higher Seebeck coefficient, lower resistivity/noise compared with poly-silicon, we finally choose SC-silicon to replace traditional poly-silicon for the thermocouple. The CS-silicon is boron doped to adjust the resistivity to about 0.0035 Ω·cm. Accordingly, aluminum serves as another material for the thermocouple.

Based on Eq. (3), sensitivity is proportional to the number of thermocouples. However, increasing the number of thermocouples cannot linearly increase sensitivity of thermopile detector, as it also simultaneously increases thermal resistance. In addition, the device will increase its thermal noise with increasing the number of thermocouples. Eventually, the thermopile detector design should be concrete application dependent, with the tradeoff among electrical resistance, thermal conductance and sensitivity well balanced. Herein we finally choose six series-connected SC-silicon/Al thermocouples to form the thermopile.

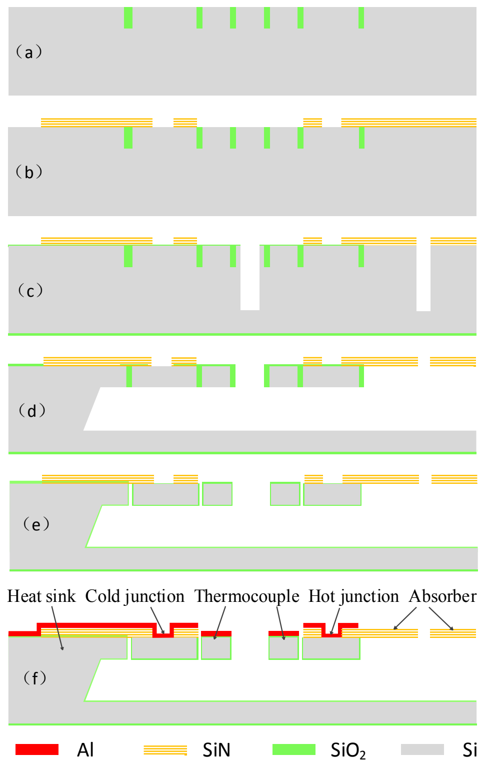

Figure 2: Fabrication process of the single-side processed bulk-micromachining thermopile.

Since the thermal resistance of the thermopile structure is proportional to the length of the thermocouple, increasing the thermocouple length is beneficial to increase sensitivity. In order to develop miniaturized IR-thermopile device without sacrificing the performance, we design a circular shape for the micromechanical structure, as is shown in Figure 1(a), which can maximize the length of the beam-shaped thermocouples within restricted area. The thermopile area is designed as small as 0.02mm^2. With this design, a circular array of 19 pixels, shown in Figure 1(b), can be adapted to a miniaturized photoreception lens that has a small diameter of 0.7mm.

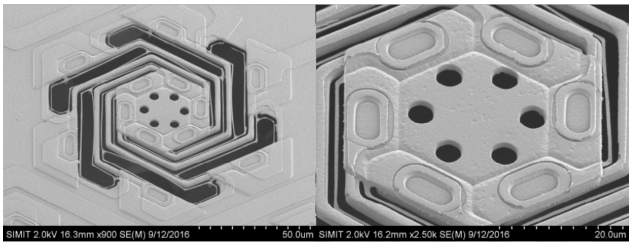

Figure 3: SEM image showing the single-side fabricated thermopile, with the magnified view at the right side to show the IR absorber area.

Single-sided micro-fabrication

Figure 2 shows the novel bulk-micromachining process that is implemented only from the front-side of (111) wafers, with which the high-sensitivity thermopiles can be low-cost fabricated compatibly in standard IC-foundries.

Firstly, narrow silicon trenches are opened in (111) wafer and then temporarily refilled with SiO_2 to define the shape of the silicon-beams. The step facilitates wafer planarization for subsequence process [Figure 2(a)]. 1.2µm-thick low-stress (LS) SiN is LPCVD deposited and patterned as the IR absorber or the bridges to connect the cold junction to heat sink [Figure 2(b)]. 200nm SiO_2 is thermally grown on the wafer surface and deeper trenches are etched by deep RIE for subsequent structure release [Figure 2(c)]. Then the cavity beneath the structure is excavated by TMAH lateral etch, which is started from alternatively opened deep trenches. After etch is automatically stopped at (111) plane, the silicon beams (served as one thermocouple material) and the central SiN film are freed [Figure 2(d)]. To avoid the influence to thermal conductance, the SiO_2 clamped by adjacent silicon beams is removed by buffered oxide etching. Before aluminum sputtering, 100nm SiO_2 is grown for electric insulation. Contact holes are opened by RIE [Figure 2(*e*)]. 600nm-thick Al film is sputtered and patterned into interconnection lines [Figure 2(f)].

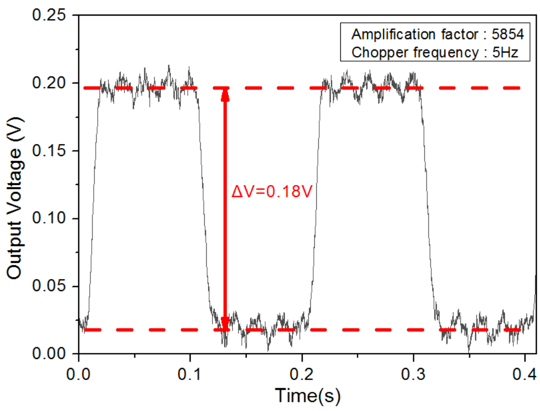

Figure 4: In-air response of the thermopile (output is 5854×amplified) is measured under 6.91mW/cm^2 IR exposure. The IR radiation is modulated by 5Hz chopper.

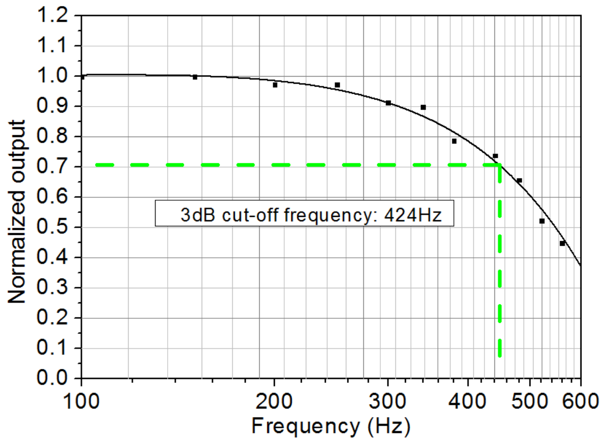

Figure 5: Measured frequency response of the thermopile, where 3dB cut-off frequency is 424 Hz.

RESULTS AND DISCUSSION

The SEM images in Figure 3 show the fabricated thermopile and the close-up view for the central IR absorber. The formed devices are tested in air with a blackbody furnace (modulated at 500K). Under 6.91mW/cm^2 IR exposure (modulated by a 5Hz chopper), the thermopile outputs 180mV voltage after 5854× amplification (see Figure 4). Therefore, an ultra-high responsivity (i.e. sensitivity) of one thermopile of 356V/W is achieved. And the normalized detectivity is also obtained as $D^*=5.54\times10^7$cm/√Hz/W. Figure 5 shows the tested frequency response. Based on the tested 3dB cut-off frequency of 424Hz, a very short response time of 0.59ms is achieved.

Table 2: Parameters of the thermopile.

Parameters	Values
Detector area	0.02mm^2
Absorber area	0.00125mm^2
Length of thermocouple beam	134µm
Cross section area of Si beam	4µm^2
Cross section area of Al line	1.2µm^2
Pair number of thermocouple	6
Resistance	31KΩ

Table 2 lists the designed and tested data for calculation. Table 3 compares the thermopile properties in this work with those reported in the representative works, indicating obvious superiority of our novel device in terms of sensitivity, response rate and miniaturization.

Table3: Characteristic data of different thermopiles.

Ref.	Area mm^2	D* 10^7cm√Hz/W	R V/W	Thermocouple materials
[8]	1.69	6.08	70	Poly/Al
[9]	1.32	6	5	p-Si/Al
[10]	1.21	/	63	Poly/Al
[11]	0.062	1.05	15	Poly/Al
[12]	0.032	5.3	37.4	Poly/Al
[13]	0.021	/	60	p-Poly/n-Poly
This work	**0.02**	**5.54**	**356**	**p-Si/Al**

CONCLUSIONS

This paper reports design, fabrication and test of the thermopiles for portable human-body/heat-source detector. The sensitivity and response time of the thermopiles are important for this application. In order to fulfill the specification requirement, a tiny-sized (140μm×140μm) p-Si/Al thermopile detecting element is designed and then bulk-micromachined only from the front-side of (111) wafer. Thanks to the novel single-side bulk-micromachined structure, the tiny-size MEMS thermopile consists of six SC-silicon/Al thermocouples and the thermocouple exhibits significantly higher Seebeck coefficient, lower resistivity and lower noise compared to the traditional poly-silicon/Al thermocouples. Te test shows that our tiny-size thermopile achieves an ultra-high responsivity of 356V/W and ultra-short response-time of 0.59ms. In the future, it is promising for us to arrange more thermopile detecting elements into an array for infrared focal plane array (IRFPA).

ACKNOWLEDGEMENTS

This work was supported by the Project of Shanghai Science and Technology Commission (14521106100), MOST of China (2016YFA0200800) and NSF of China (91323304, 61527818, 61321492).

REFERENCES

[1] J. Tanaka, M. Shiozaki, F. Aita, et al, “Thermopile infrared array sensor for human detector application”, Proc. IEEE MEMS 2014, 2014, pp.1213-1216.

[2] T. Ishikawa, M. Ueno, Y. Nakaki, et al, “Performance of 320×240 uncooled IRFPA with SOI diode detectors”, Proc. SPIE 4130, 2000, pp. 152-159.

[3] M. Hirota, Y. Nakajima, M. Saito, et al, “120×90 element thermoelectric infrared focal plane array with precisely patterned Au-black absorber”, Sens. Actuators A, vol. 135, pp. 146-151, 2007.

[4] C. Escriba, E. Campo, D. Esteve, et al, “Complete analytical modeling and analysis of micromachined thermoelectric uncooled IR sensors”, Sens. Actuators A, vol. 120, pp. 267-276, 2005.

[5] D. Xu, B. Xiong, Y. Wang, “Design fabrication and characterization of a front-etched micromachined thermopile for IR detection”, J. Micromech. Microeng., vol. 20, pp. 115004, 2010.

[6] D.R.Lide (Ed.), CRC Handbook of Chemistry and physics, 81 st edition, CRC Press, Boca Raton, FL, 2000.

[7] R. Muanghlua, S. Cheirsirikul, S. Supadech, “The study of silicon thermopile”, Proc. IEEE *TENCON 2000*, 2000, vol. 3, pp. 226-229.

[8] D. Xu, B. Xiong, Y. Wang, et al, “Hybrid etching process and its application in thermopile infrared sensor”, Proc. IEEE NEMS 2010, 2010, pp. 425-428.

[9] P. M. Sarro, H. Yashiro, A. W. Herwaarden, et al, “An integrated thermal infrared sensing array”, Sens. Actuators A, vol. 14, pp. 191-201, 1988.

[10] S. J. Chen, C. H. Shen. “A new high-filling-factor CMOS-compatible thermopile”, IEEE T. Instrum. Meas., 2007, vol.56, pp.231-1238.

[11] C. Calaza, N. Viarani, G. Pedretti, et al, “An uncooled infrared focal plane array for low-cost applications fabricated with standard CMOS technology”, Sens. Actuators A, vol. 132, pp. 129-138, 2006.

[12] C.H. Du and Ch.K. Lee, “3D thermoelectric structures derived from a new mixed micromachining process”, Jpn. J. Appl. Phys., vol. 39, pp. 7125, 2000.

[13] M. Hirota, Y. Ohta, Y. Fukuyama, “Low-cost thermo-electric infrared FPAs and their automotive applications”, Proc. SPIE, 2008, pp. 694032.

CONTACT

X.X. Li, tel: +86-21-62131794; xxli@mail.sim.ac.cn